Published on 12 February 2014. Downloaded by ECOLE POLYTECHNIC FED DE LAUSANNE on 01/01/2015 22:20:11.

PCCP

PAPER

View Article Online
View Journal | View Issue

# Nanoporous molybdenum carbide wires as an active electrocatalyst towards the oxygen reduction reaction

Cite this: *Phys. Chem. Chem. Phys.*, 2014, **16**, 10088

Lei Liao,[ab] Xiaojun Bian,[a] Jingjing Xiao,[a] Baohong Liu,*[a] Micheál D. Scanlon[b] and Hubert H. Girault*[b]

Received 10th November 2013,
Accepted 29th January 2014

DOI: 10.1039/c3cp54754j

www.rsc.org/pccp

A non-precious metal electrocatalyst has been developed for the oxygen reduction reaction based on nanoporous molybdenum carbide (nano-$Mo_2C$) wires through a facile calcination of sub-nanometer periodic organic–inorganic hybrid nanowires. The highly dispersed $Mo_2C$ wires were composed of 10–15 nm nanocrystals with a mesopore size of 3.3 nm. The properties of nano-$Mo_2C$ wires were characterized using scanning electron microscopy, transmission electron microscopy, X-ray diffraction and $N_2$ adsorption/desorption porosimetry. The highly active surface area and enriched nanoporosity for nano-$Mo_2C$ wires are unique features that make them a high-performance electrocatalyst for oxygen reduction in an alkaline medium. The electrocatalysis and reaction kinetics results show that nano-$Mo_2C$-based materials can be developed as new catalysts with high activity at low cost for electrochemical energy conversion applications.

## 1. Introduction

The field of energy conversion and storage has been the subject of increased research effort in recent years. In particular the oxygen reduction reaction (ORR) at the cathode in fuel cells has attracted considerable attention.[1–3] Platinum (Pt) and its alloys are the most effective electrocatalysts for the ORR; however, as Pt-based catalysts are expensive and of low abundance, this limits their large-scale applicability in many fields.[4–6] The development of efficient ORR catalysts that can replicate the catalytic activity of Pt-based materials remains challenging and much effort has been devoted in this direction. Non-precious metals and metal-free materials including non-pyrolyzed and pyrolyzed transition metal nitrogen-containing complexes,[7] transition metal chalcogenides,[8] metal oxides[9,10]/carbides[11]/nitrides,[12] N-doped graphene[13] or mesoporous carbon nitrides,[14] and enzymatic compounds[15] have been actively pursued as alternative electrocatalysts. Among these candidates, pyrolyzed transition metal nitrogen-containing complexes are considered to be the most promising ORR catalysts because they have demonstrated ORR activity and stability close to that of commercially available Pt/C catalysts. Although great progress has been achieved in this field, it is still challenging but desirable to develop efficient catalysts for the ORR. Transition metal carbides often display electronic and catalytic properties that are similar to those of Pt-group metals.[16] Following the pioneering work of Hu *et al.*,[17] our groups have demonstrated that molybdenum carbides are active catalysts for the hydrogen evolution reactions both on modified electrodes and at soft interfaces.[18–20] Their highly attractive physicochemical properties, originating from the unique metal–carbon chemical bonds and noble-metal-like d-state density around the Fermi level, of thermal stability, mechanical hardness and high catalytic performance in hydrocarbon conversion, has led to them being carefully scrutinized as promising ORR catalysts.[21,22]

Herein, we propose a nano-sized $Mo_2C$ wire that acts as an advanced electrocatalyst towards the oxygen reduction reaction. To realize this purpose, the nanoporous molybdenum carbide wires were prepared through a facile calcination of sub-nanometer periodic organic–inorganic hybrid nanowires and successfully demonstrated a high ORR performance. The unique features of such $Mo_2C$ wires, including high active surface areas and enriched nanoporosity, lead not only to more exposed edge sites for catalysis but also facilitate highly efficient dispersion in a reaction solution. Both of these factors lead to a high electrocatalytic activity towards ORR and stability in an alkaline medium. As the structure of these nano-$Mo_2C$ wires is different from that of commercial catalysts, our insights may lead to new theoretical and experimental investigations regarding molybdenum-containing ORR catalysts.

[a] *Department of Chemistry, State Key Lab of Molecular Engineering of Polymers and Collaborative Innovation Center of Chemistry for Energy Materials, Fudan University, Shanghai 200433, P. R. China. E-mail: bhliu@fudan.edu.cn*
[b] *Laboratoire d'Electrochimie Physique et Analytique, École Polytechnique Fédérale de Lausanne, CH-1015 Lausanne, Switzerland. E-mail: hubert.girault@epfl.ch*


This journal is © the Owner Societies 2014

Published on 12 February 2014. Downloaded by ECOLE POLYTECHNIC FED DE LAUSANNE on 01/01/2015 22:20:11.

# 2. Experimental

## 2.1. Reagents

Ammonium heptamolybdate ($(NH_4)_6Mo_7O_{24}\cdot 4H_2O$), aniline, commercial $Mo_2C$, Vulcan carbon and Nafion® perfluorinated ion-exchange resin solution (5% w/w), Pt/C (10 wt% platinum on Vulcan carbon) were purchased from Sigma-Aldrich. Other reagents were obtained from the Shanghai Chemical Plant. Ethanol, methanol and KOH were obtained from the Shanghai Chemical Plant. All aqueous solutions were prepared using ultrapure water.

## 2.2. Synthesis of nano-$Mo_2C$ wires

Nanoporous $Mo_2C$ wires were prepared according to our previous report with some modifications.[18,23] The precursor of $Mo_3O_{10}(C_6H_8N)_2\cdot 2H_2O$ was first synthesized through a facile method. Typically, 2.48 g of ammonium heptamolybdate and 3.2 g of aniline were added to 40 mL of distilled water. Next an aqueous solution of 1.0 M HCl was added drop-wise, with magnetic stirring at room temperature, until a white precipitate appeared (the pH was approximately 4 to 5). After stirring at 50 °C for 5 hours, the product was filtered, washed with ethanol and dried at 50 °C for 10 hours. After expelling air for 4 hours at room temperature using argon, the obtained precursor was calcinated at 725 °C for 5 hours under an argon flow to obtain the nano-$Mo_2C$ wire catalyst. Considering that Pt may influence the catalytic results,[24] Pt crucibles were not used at any stage during the synthesis processes and, additionally, the porcelain crucible used was never exposed to any Pt metal or Pt containing species.

## 2.3. Characterization

The morphology of nano-$Mo_2C$ wires was characterized using scanning electron microscopy (SEM, Philips XL 30) at 10 keV and transmission electron microscopy (TEM, JEOL JEM-2011 electron microscope) at an acceleration voltage of 200 keV. X-ray diffraction (XRD) patterns were obtained on a Bruker D8 Advance. Nitrogen adsorption/desorption isotherms were collected with the aid of Quantachrome's Quadrasorb SI analyzer at 77 K. Prior to measurements, the samples were degassed at 523 K for 3 hours under vacuum. The Brunauer–Emmett–Teller (BET) method was used to calculate the specific surface area. The pore size distribution was analysed by the thermodynamics-based Barrett–Joyner–Halenda (BJH) method[25] with a spherical pore model on the adsorption branch of the isotherms. The total pore volume was calculated from the adsorbed amount at a maximum relative pressure of $P/P_0$.

## 2.4. Electrochemical measurements

Electrochemical measurements were carried out on a CHI660C electrochemical workstation (CH instruments, Texas, USA). A platinum wire and a saturated calomel electrode (SCE) were used as the counter and reference electrodes, respectively. For rotating disk electrode (RDE) measurements, PINE research instrumentation (USA) was used and a glassy carbon disk electrode (GCE) acted as the working electrode (5 mm diameter). The GCE was modified with 10 μL of 4 mg $mL^{-1}$ nano-$Mo_2C$ wire catalyst suspensions in water and ethanol (w/w = 4 : 1 containing 80 μL of 5 wt% Nafion per mL). The modified GCE was left to dry at room temperature. For comparison, GCEs were modified with commercial $Mo_2C$ catalysts, Pt/C (10 wt% platinum on Vulcan carbon, Sigma) and nano-$Mo_2C$ wires physically mixed with Vulcan carbon. Each modified GCE was loaded with an identical amount of $Mo_2C$ (0.21 mg $cm^{-2}$). For all electrochemical measurements, oxygen saturated 0.1 M KOH aqueous solutions were used as the electrolyte and a flow of oxygen maintained over the electrolyte for the duration of each measurement in order to ensure continuous oxygen saturation. Prior to each measurement, a resistance test was performed and *iR* compensation applied using the CHI software. The electrocatalytic activity of nano-$Mo_2C$ wires towards the ORR was determined by polarization curves using linear sweep voltammetry (LSV) at a scan rate of 10 mV $s^{-1}$. LSV was performed at various rotation rates from 400 rpm to 2025 rpm. Cyclic voltammograms (CVs) were recorded at a scan rate of 50 mV $s^{-1}$. The working electrode was cycled at least five times for activation in oxygen saturated 0.1 M KOH aqueous solutions before data were recorded. During control experiments, CV measurements were also performed under anaerobic conditions by switching to a nitrogen flow through the electrochemical cell. All electrochemical data were collected at room temperature (25 °C), maintained using a thermostatic water bath.

# 3. Result and discussion

## 3.1. Synthesis and characterization of nano-$Mo_2C$ wires

The nanoporous $Mo_2C$ wires were prepared by calcinating organic–inorganic hybrid $Mo_3O_{10}(C_6H_8N)_2\cdot 2H_2O$ nanowire precursors at 725 °C under an argon flow.[18] The intercalating amine molecules act as both the reducing agent and the source of carbon in this reaction. Fig. 1A depicts a scanning electron microscopy (SEM) image of nano-$Mo_2C$ where the wire-like products of uniform morphology, several micrometers in length

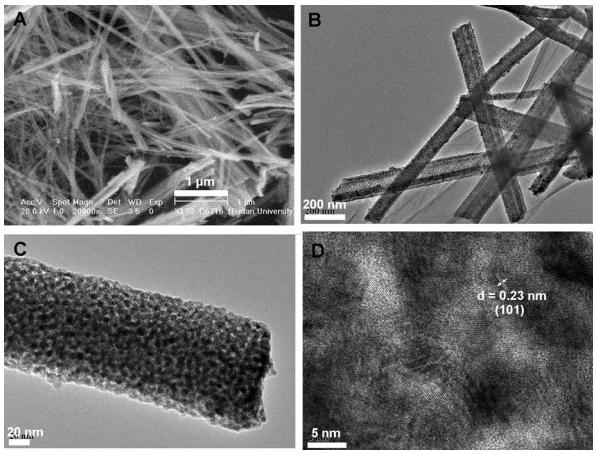


Fig. 1 SEM (A) and TEM (B, C) images of nano-$Mo_2C$ wires. (D) High-resolution TEM image of nano-$Mo_2C$ wires confirming that such wires are composed of nanoparticles.

Published on 12 February 2014. Downloaded by ECOLE POLYTECHNIC FED DE LAUSANNE on 01/01/2015 22:20:11.

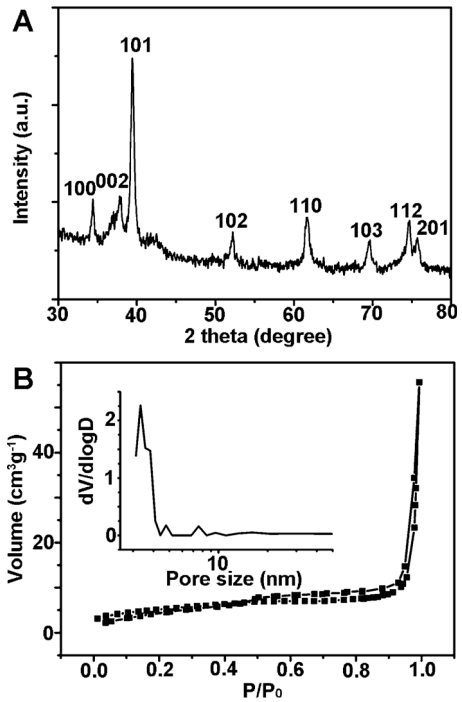


Fig. 2 (A) XRD pattern and (B) $N_2$ adsorption/desorption isotherm of nano-$Mo_2C$ wires.

and 80–150 nm in width, were observed. The transmission electron microscopy (TEM) images (Fig. 1B) confirmed their highly dispersed morphologies with individual wires. A high-resolution TEM image (Fig. 1C and D) highlights the formation of a crystalline framework composed of 10–15 nm nanocrystallites. The orientation (101) of the $Mo_2C$ nanocrystals agrees with that indicated by the XRD pattern in Fig. 2A, which are confirmed to be the hexagonal phase (JCPDS: 35-0787). The aggregation of the $Mo_2C$ nanocrystallites inside the wires leads to a BET surface area of 53.3 $m^2\ g^{-1}$ and a pore size of 3.3 nm in diameter, as confirmed by a $N_2$ sorption isotherm (Fig. 2B).

### 3.2. Electrocatalytic properties toward the ORR

The electrocatalytic properties of commercial $Mo_2C$ and nano-$Mo_2C$ wires were compared with that of both bare and commercial Pt–C (10 wt% platinum on Vulcan carbon) modified glassy-carbon rotating-disk electrodes (GC-RDE, 5 mm diameter) in oxygen or nitrogen saturated 0.1 M KOH solutions using a three-electrode setup. The same amount of each catalyst by mass (0.21 mg $cm^{-2}$) was loaded onto each GC-RDE. Polarisation curves of GC-RDEs modified with various catalysts, as noted, are shown in Fig. 3A and B. Firstly, the activity of a bare GC-RDE was substantially less than that of a nano-$Mo_2C$ wires modified GC-RDE (Fig. 3A). The nano-$Mo_2C$ wires showed a considerably more positive ORR onset potential (at approximately 0.87 V *vs.* RHE) than both the bare GC-RDE (Fig. 3A) and that modified by commercial $Mo_2C$ particles (Fig. 3B). Indeed, the onset potential of the nano-$Mo_2C$ wires modified GC-RDE was close to that identified from CV measurements (0.86 V *vs.* RHE, Fig. 3B and C). Meanwhile, the Pt–C catalyst modified GC-RDE showed better catalytic activity with an onset potential of 0.99 V (*vs.* RHE) corroborating the existing literature on this catalyst.[5,6] In order to confirm the reproducibility of the catalytic responses for each modified GC-RDE, five individual electrodes were tested. An average current density at 0.4 V (*vs.* RHE) of −2.94 mA $cm^{-2}$ was obtained at a rotation rate of 1600 rpm. The relative standard deviation was approximately 1.4% for these measurements, thereby confirming the reproducibility of the catalytic response. Fig. 3C and D present CVs of a nano-$Mo_2C$ wire modified GCE and a Pt–C modified GCE, respectively, in oxygen or nitrogen saturated 0.1 M KOH solutions at a scan rate of 50 mV $s^{-1}$. Featureless voltammetric responses were observed for a nano-$Mo_2C$ wire modified GCE in nitrogen saturated solutions within the studied potential range. In contrast, when the electrolyte solution was saturated with oxygen, the reduction current appeared as a well-defined cathodic peak at 0.76 V (*vs.* RHE), suggesting a pronounced electrocatalytic activity of the nano-$Mo_2C$ wire modified GCE for oxygen reduction.

To examine possible crossover effects, we measured the electrocatalytic selectivity of nano-$Mo_2C$ wire modified and Pt–C modified GCEs against the electrooxidation of methanol in oxygen-saturated 0.1 M KOH. For a Pt–C modified GCE in the presence of methanol (3.0 M), the obtained CV exhibited one pair of peaks for methanol oxidation, whereas the cathodic peak for ORR had vanished (Fig. 3D). However, with a nano-$Mo_2C$ wire modified GCE, no noticeable change was observed in the oxygen-reduction current under the same conditions (Fig. 3C). Thus, nano-$Mo_2C$ wires exhibited high selectivity for the ORR, with a remarkably good ability to avoid crossover effects and outperformed the Pt–C catalyst. Such $Mo_2C$ nanowires may hold promise for use in direct methanol and alkaline fuel cells.

### 3.3. Kinetics and stability study

The reaction kinetics were further studied to gain insights into the role of nano-$Mo_2C$ wires during the ORR electrochemical process. The voltammetric profiles in an oxygen saturated 0.1 M KOH solution showed that the current density was enhanced upon increasing the rotation rates (from 400 rpm to 2025 rpm, Fig. 4A). The corresponding Koutecky–Levich plots ($J^{-1}$ *vs.* $\omega^{-1/2}$) at various electrode potentials exhibited good linearity (Fig. 4B). The kinetic parameters can be analyzed on the basis of the Koutecky–Levich (K–L) equations.[26–28]

$$J^{-1} = J_L^{-1} + J_K^{-1} \quad (1)$$

$$J_L = 0.62nFC_0D^{2/3}\nu^{-1/6}\omega^{1/2} \quad (2)$$

$$J_K = nFkC_0 \quad (3)$$

where $J$ is the current density, $J_K$ and $J_L$ are the kinetic- and diffusion-limiting current densities, $\omega$ is the angular velocity of the disk ($\omega = 2\pi N$, $N$ being the rotation frequency), $n$ is the overall number of electrons transferred upon oxygen reduction, $F$ is the Faraday constant ($F$ = 96 485 C $mol^{-1}$), $D$ is the diffusion coefficient of $O_2$ in 0.1 M KOH electrolyte ($1.9 \times 10^{-5}$ $cm^2\ s^{-1}$), $C_0$ is the bulk concentration of $O_2$ ($1.2 \times 10^{-3}$ mol $L^{-1}$), $\nu$ is the

 This journal is © the Owner Societies 2014

Published on 12 February 2014. Downloaded by ECOLE POLYTECHNIC FED DE LAUSANNE on 01/01/2015 22:20:11.

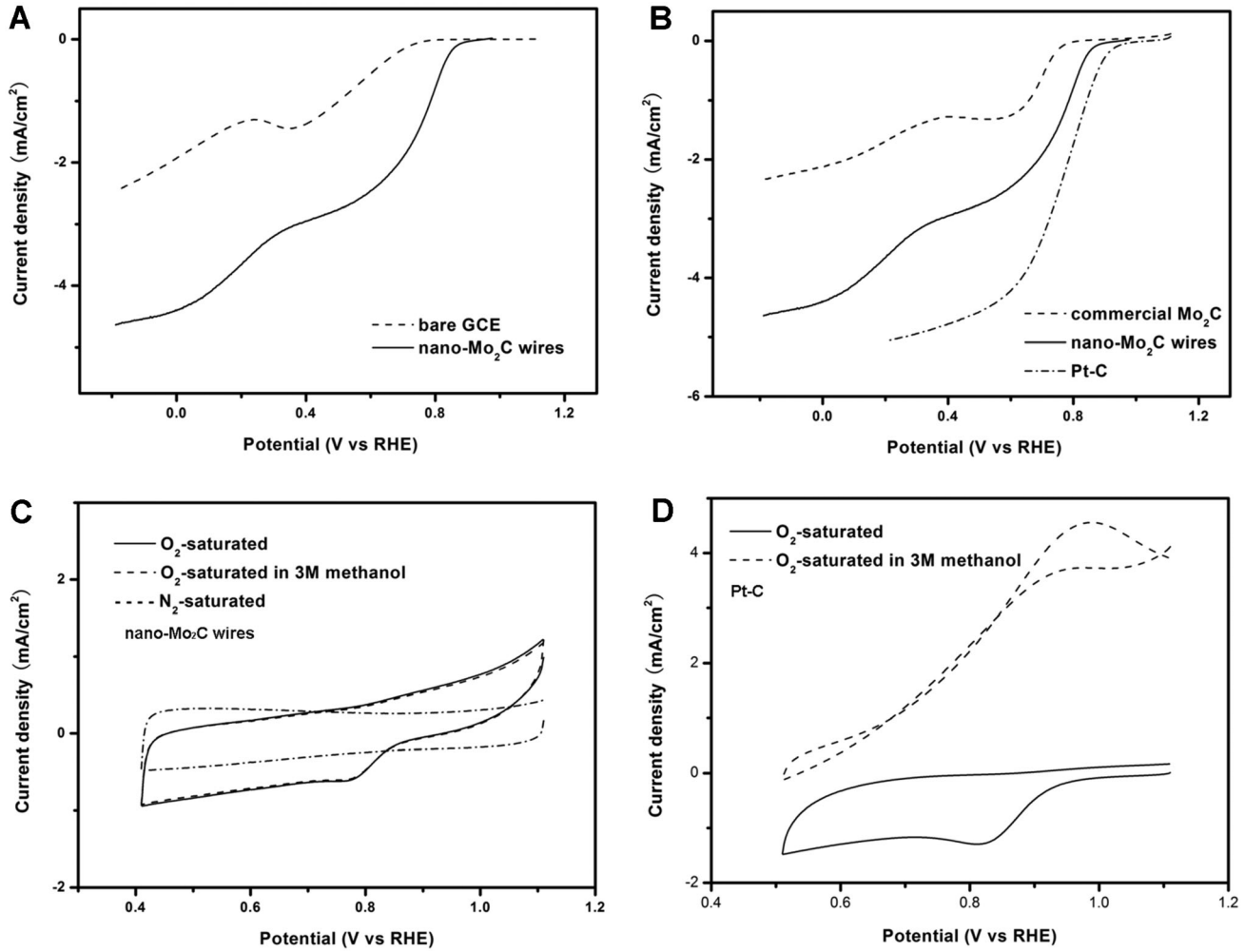


Fig. 3 Polarisation curves of (A) bare and nano-$Mo_2C$ wire modified GC-RDEs and (B) commercial $Mo_2C$, nano-$Mo_2C$ wire and Pt–C modified GC-RDEs. The LSV experiments were performed with a rotation rate of 1600 rpm, at a scan rate of 10 mV $s^{-1}$, in an oxygen saturated 0.1 M KOH solution. CVs of (C) nano-$Mo_2C$ wires and (D) Pt–C modified GC-RDEs in an oxygen saturated 0.1 M KOH solution, an oxygen saturated 0.1 M KOH solution with the addition of methanol (3.0 M), and a nitrogen saturated 0.1 M KOH solution. Scan rate: 50 mV $s^{-1}$.

kinetic viscosity of the electrolyte (0.01 $cm^2$ $s^{-1}$) and $k$ is the electron transfer rate constant. According to the K–L plots, the average electron transfer number $n$ for nano-$Mo_2C$ wires towards the ORR is 3 over the potential range from 0.7 V to 0.4 V (*vs.* RHE) and 4 over the potential range from 0.3 V to 0 V (*vs.* RHE). This suggests that the ORR process at a nano-$Mo_2C$ catalyst is a combination of two-electron and four-electron pathways or a two-step two-electron process with the formation of intermediate $HO_2^-$ ions as indicated by two reduction waves starting at ~0.87 V and ~0.41 V (*vs.* RHE), respectively.[13]

Tafel analysis was also performed to gain information about the oxygen adsorption mechanism on nano-$Mo_2C$ wire modified GC-RDEs. Diffusion-corrected Tafel plots were employed to eliminate the impact of diffusion on the adsorption kinetic analysis by plotting the potentials ($E$) as a function of the absolute values of the kinetic currents ($|J_k|$) in a semi-logarithmic form (Fig. 4C). In the low-overpotential region (>0.8 V), where the overall ORR speed is determined by the surface reaction rate on the catalyst, the Tafel slope for nano-$Mo_2C$ wires is ~65 mV per decade (from 0.87 V to 0.83 V *vs.* RHE), which is very close to the value for a Pt/C catalyst (~64 mV per decade).[29,30] Additionally, the nano-$Mo_2C$ wires exhibit comparable stability to a Pt–C catalyst in oxygen saturated 0.1 M KOH solutions with 13% decay in ORR activity over 25 000 s (Fig. 5). Pt catalysts are known to gradually degrade over time because of the irreversible formation of surface oxides and particle dissolution and aggregation, especially in the alkaline electrolytes used for fuel cells. As the lack of catalyst stability is one of the major challenges facing alkaline fuel cells, exploring routes to develop more durable catalysts for the ORR in alkaline solutions is a priority.[9]

The precise nature of the catalytic sites for the ORR with $Mo_2C$-based materials is still a matter of debate. Previously, Vrubel and Hu[17] have shown that the surface of $Mo_2C$ particles are contaminated with molybdenum oxides, such as $MoO_3$ and $MoO_2$, prior to electrochemical activation. We have also found this to be the case from preliminary X-ray photoelectron spectroscopy (XPS) of our nano-$Mo_2C$ wires (not shown). In addition,

Published on 12 February 2014. Downloaded by ECOLE POLYTECHNIC FED DE LAUSANNE on 01/01/2015 22:20:11.

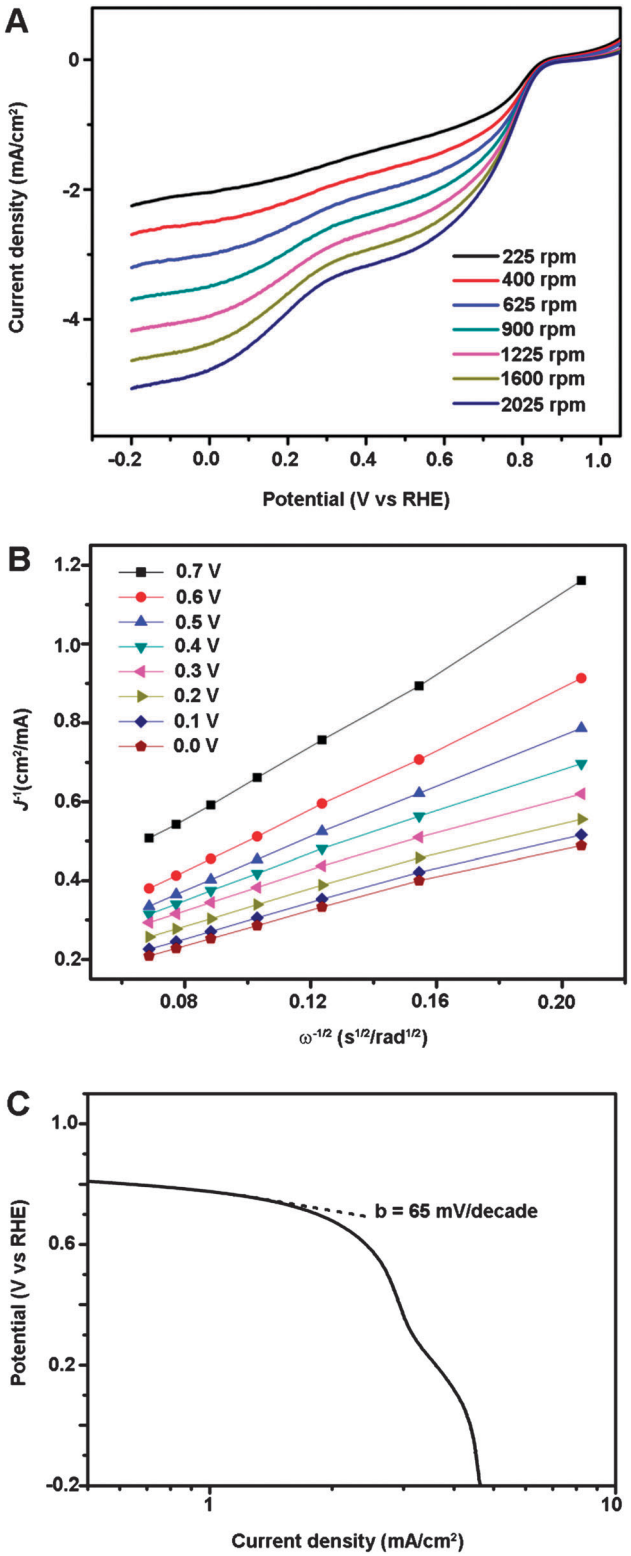


Fig. 4 (A) Polarisation curves of a nano-$Mo_2C$ wire modified GC-RDE with various rotation rates at a scan rate of 10 mV $s^{-1}$ in an oxygen saturated 0.1 M KOH solution. (B) The Koutecky–Levich plots of $J^{-1}$ *versus* $\omega^{-1/2}$ deduced from the data of (A) at different potentials. (C) Tafel plot of nano-$Mo_2C$ derived by the mass-transport correction of the corresponding rotating disk electrode data.

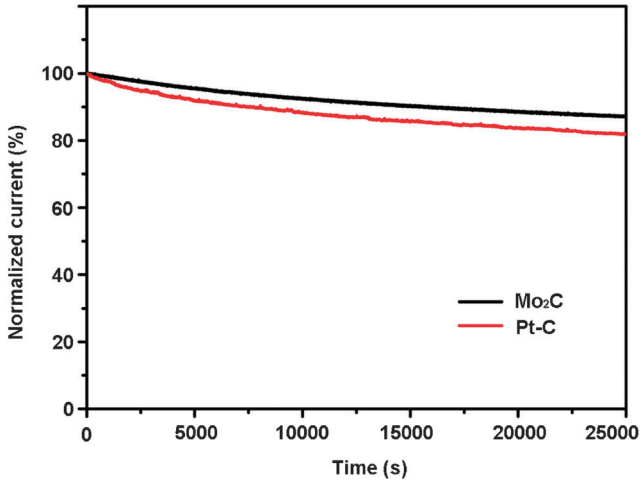


Fig. 5 Chronoamperometric response of nano-$Mo_2C$ wires and Pt–C kept at 0.6 V (*vs.* RHE) in an oxygen saturated 0.1 M KOH solution.

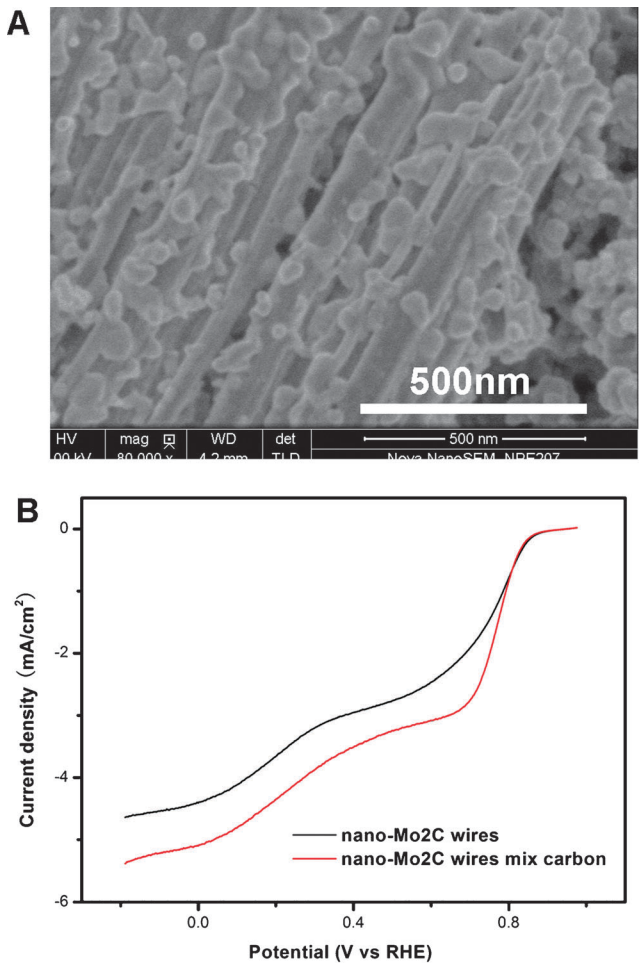


Fig. 6 (A) SEM image of nano-$Mo_2C$ wires physically mixed with Vulcan carbon. (B) Polarisation curves of nano-$Mo_2C$ wires, mixed nano-$Mo_2C$/carbon catalyst modified GC-RDEs with a rotation rate of 1600 rpm, at a scan rate of 10 mV $s^{-1}$, in an oxygen saturated 0.1 M KOH solution.


This journal is © the Owner Societies 2014

Published on 12 February 2014. Downloaded by ECOLE POLYTECHNIC FED DE LAUSANNE on 01/01/2015 22:20:11.

Vrubel and Hu noted that, firstly, the amounts of $MoO_3$ and $MoO_2$ diminished greatly after activation by Galvanostatic electrolysis for short periods of time and, secondly, that $MoO_2$, $MoO_3$ and Mo metal are not efficient catalysts for the hydrogen evolution reaction (HER).[17] Accordingly, a future perspective of this work will be to perform a more in-depth investigation to determine the precise nature of the true catalytic sites for the ORR after $Mo_2C$ activation, *i.e.*, are they $Mo_2C$ itself, molybdenum oxides or, perhaps, molybdenum oxycarbide species. This work will be predominantly based on in-depth XPS analysis using a custom setup (with extreme care necessary to prevent activated electrode surfaces being re-oxidised by exposure to air) and theoretical approaches using density functional theory (DFT) calculations.

### 3.4. Electrocatalytic properties of a $Mo_2C$–carbon composite toward the ORR

Moreover, it is known that the morphology and electrical conductivity of catalysts are important factors affecting the electrocatalytic efficiency. Considering that carbon materials are ideal supports to improve the electrocatalytic activity, here the nano-$Mo_2C$ wires and commercial Vulcan carbon ($Mo_2C$/carbon) were further physically mixed to modify a GC-RDE. Fig. 6B indicated that the catalytic current density was enhanced compared with that of pure nano-$Mo_2C$ wire catalysts. This could be attributed to the improved conductivity due to the contact of nano-$Mo_2C$ wires with the carbon, which afforded facilitated electron transfer between the $Mo_2C$/carbon and the electrode.[17] SEM images (Fig. 6A) confirmed the close nature of this interaction highlighting the distribution of the carbon nanoparticles and their attachment to the $Mo_2C$ wires. The LSV curves measured with mixed nano-$Mo_2C$/carbon catalyst modified GC-RDE at various rotation speeds are presented in Fig. 7A, showing increased cathodic current at increased rotation speeds due to improved mass transport at the electrode surface. From the slope of the Koutecky–Levich plots obtained from the data in Fig. 7A, the number of electrons per oxygen molecule in the ORR is calculated to be 3 over the potential range from 0.7 V to 0.4 V (*vs.* RHE) and 4 over the potential range from 0.3 V to 0 V (*vs.* RHE) (Fig. 7B), consistent with the results of nano-$Mo_2C$ wires. Similar catalytic mechanisms may occur in both systems in the present study. This proof-of-concept experiment showed that supporting nano-sized $Mo_2C$ on functional carbon matrices could be expected to improve the electronic conductivity and catalyst dispersibility, thus promoting the electrocatalytic activity by synergetic effects. Future perspectives will focus on *in situ* formation of $Mo_2C$ nanocomposites on various carbon supports as advanced electrocatalysts for oxygen reduction reactions.

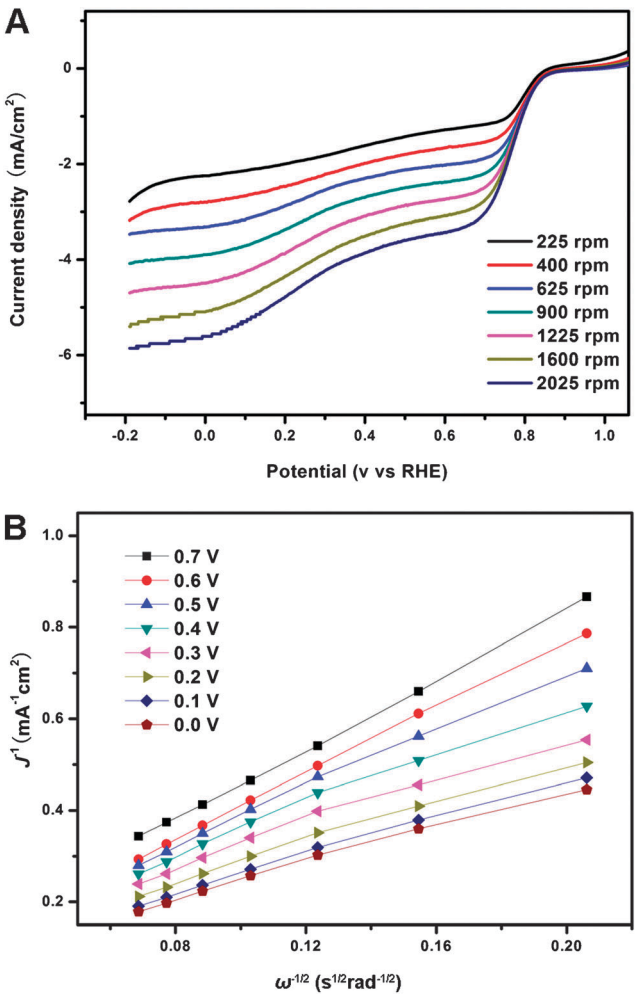


Fig. 7 (A) Polarisation curves of mixed nano-$Mo_2C$/carbon catalyst modified GC-RDE with various rotation rates at a scan rate of 10 mV $s^{-1}$ in an oxygen saturated 0.1 M KOH solution. (B) The Koutecky–Levich plots of $J^{-1}$ *versus* $\omega^{-1/2}$ deduced from the data of (A) at different potentials.

## 4. Conclusions

In conclusion, nanoporous molybdenum carbide wires have been synthesized using a simple, cost-effective and safe approach. The special features of nano-$Mo_2C$ wires are their enriched nanoporosity and large active surface areas that accelerate the interfacial electrochemical reaction, contributing to their potent ORR activity. The resulting nano-$Mo_2C$ wires are shown to be efficient catalysts towards the oxygen reduction reaction showing high electrocatalytic activity, excellent resistance to crossover effects and comparable stability towards the ORR to another well known, but precious metal containing, Pt–C catalyst. Additionally, proof-of-concept results show that the catalytic performance could be further improved through supporting the nanoparticles of $Mo_2C$ on functional carbon materials with synergistic effects, which may open up a new road to advanced catalysts for energy conversion and storage.

## Acknowledgements

This work was supported by NSFC 20925517, SKLEAC201101 and Swiss Science Foundation grant 200 021-134 745.

Published on 12 February 2014. Downloaded by ECOLE POLYTECHNIC FED DE LAUSANNE on 01/01/2015 22:20:11.

## References

1 B. C. H. Steele and A. Heinzel, *Nature*, 2001, **414**, 346–352.
2 N. S. Lewis and D. G. Nocera, *Proc. Natl. Acad. Sci. U. S. A.*, 2006, **103**, 15729–15735.
3 Q. Li, M. C. Henstridge, C. B. McAuley, N. S. Lawrence, R. S. Hartshorne and R. G. Compton, *Phys. Chem. Chem. Phys.*, 2013, **15**, 7854–7865.
4 A. C. Garcia and E. A. Ticianelli, *Electrochim. Acta*, 2013, **106**, 453–459.
5 Y. Li, Y. Li, E. Zhu, T. McLouth, C.-Y. Chiu, X. Huang and Y. Huang, *J. Am. Chem. Soc.*, 2012, **134**, 12326–12329.
6 B. Lim, M. Jiang, P. H. C. Camargo, E. C. Cho, J. Tao, X. Lu, Y. Zhu and Y. Xia, *Science*, 2009, **324**, 1302–1305.
7 Z. Chen, D. Higgins, A. Yu, L. Zhang and J. Zhang, *Energy Environ. Sci.*, 2011, **4**, 3167–3192.
8 M.-R. Gao, J. Jiang and S.-H. Yu, *Small*, 2012, **8**, 13–27.
9 Y. Liang, Y. Li, H. Wang, J. Zhou, J. Wang, T. Regier and H. Dai, *Nat. Mater.*, 2011, **10**, 780–786.
10 Y. Liang, H. Wang, J. Zhou, Y. Li, J. Wang, T. Regier and H. Dai, *J. Am. Chem. Soc.*, 2012, **134**, 3517–3523.
11 X. Li, D. Ma, L. Chen and X. Bao, *Catal. Lett.*, 2007, **116**, 63–69.
12 Y. Li, T. Takata, D. Cha, K. Takanabe, T. Minegishi, J. Kubota and K. Domen, *Adv. Mater.*, 2013, **25**, 125–131.
13 B. Zheng, J. Wang, F.-B. Wang and X.-H. Xia, *Electrochem. Commun.*, 2013, **28**, 24–26.
14 K. Kwon, Y. J. Sa, J. Y. Cheon and S. H. Joo, *Langmuir*, 2012, **28**, 991–996.
15 Y. C. Weng, F.-R. F. Fan and A. J. Bard, *J. Am. Chem. Soc.*, 2005, **127**, 17576–17577.
16 S.-H. Jhi, J. Ihm, S. G. Louie and M. L. Cohen, *Nature*, 1999, **399**, 132–134.
17 H. Vrubel and X. L. Hu, *Angew. Chem., Int. Ed.*, 2012, **51**, 12703–12706.
18 L. Liao, S. Wang, J. Xiao, X. Bian, Y. Zhang, M. D. Scanlon, X. Hu, Y. Tang, B. Liu and H. H. Girault, *Energy Environ. Sci.*, 2014, **7**, 387–392.
19 X. Bian, M. D. Scanlon, S. Wang, L. Liao, Y. Tang, B. Liu and H. H. Girault, *Chem. Sci.*, 2013, **4**, 3432–3441.
20 M. D. Scanlon, X. Bian, H. Vrubel, V. Amstutz, K. Schenk, X. Hu, B. Liu and H. H. Girault, *Phys. Chem. Chem. Phys.*, 2013, **15**, 2847–2857.
21 V. G. Pol, S. V. Pol and A. Gedanken, *Eur. J. Inorg. Chem.*, 2009, 709–715.
22 R. Jäger, P. E. Kasatkin, E. Härk and E. Lust, *Electrochem. Commun.*, 2013, **35**, 97–99.
23 Q. Gao, C. Zhang, S. Xie, W. Hua, Y. Zhang, N. Ren, H. Xu and Y. Tang, *Chem. Mater.*, 2009, **21**, 5560–5562.
24 R. H. Crabtree, *Chem. Rev.*, 2012, **112**, 1536–1554.
25 E. P. Barrett, L. G. Joyner and P. P. Halenda, *J. Am. Chem. Soc.*, 1951, **73**, 373–380.
26 L. Qu, Y. Liu, J.-B. Baek and L. Dai, *ACS Nano*, 2010, **4**, 1321–1326.
27 W. Chen and S. Chen, *Angew. Chem., Int. Ed.*, 2009, **48**, 4386–4389.
28 A. J. Bard and L. R. Faulkner, *Electrochemical Methods: Fundamentals and Applications*, Wiley, New York, 2001.
29 J. Liang, Y. Zheng, J. Chen, J. Liu, D. Hulicova-Jurcakova, M. Jaroniec and S. Z. Qiao, *Angew. Chem., Int. Ed.*, 2012, **51**, 3892–3896.
30 Z. Chen, D. Higgins, H. Tao, R. S. Hsu and Z. Chen, *J. Phys. Chem. C*, 2009, **113**, 21008–21013.

 This journal is © the Owner Societies 2014